WILEY | JCN RESEARCH IN SYSTEMS NEUROSCIENCE THE JOURNAL OF COMPARATIVE NEUROLOGY

RESEARCH ARTICLE

Age-related central regulation of orexin and NPY in the short-lived African killifish *Nothobranchius furzeri*

Alessia Montesano[1,2] | Mario Baumgart[2] | Luigi Avallone[1] | Luciana Castaldo[1] | Carla Lucini[1] | Eva Terzibasi Tozzini[3] | Alessandro Cellerino[2,3] | Livia D'Angelo[1,4] | Paolo de Girolamo[1]

[1]Department of Veterinary Medicine and Animal Productions, University of Naples Federico II, Naples, Italy

[2]Leibniz-Institute on Aging – Fritz Lipmann Institute (FLI), Lab. Biology of Aging, Jena, Germany

[3]Scuola Normale Superiore, Bio@SNS, c/o Istituto di Biofisica del CNR, Pisa, Italy

[4]Stazione Zoologica Anton Dohrn, Biology and Evolution of Marine Organisms, Naples, Italy

Correspondence
Livia D'Angelo, via F. Delpino, 1, Naples I-80137, Italy.
Email: livia.dangelo@unina.it

Funding information
University of Naples Federico II

Abstract

Orexin A (OXA) and neuropeptide Y (NPY) are two hypothalamic neuropeptides involved in the regulation of feeding behavior and food intake in all vertebrates. Accumulating evidences document that they undergo age-related modifications, with consequences on metabolism, sleep/wake disorders and progression of neurodegenerations. The present study addressed the age related changes in expression and distribution of orexin A (its precursor is also known as hypocretin—*HCRT*) and NPY, and their regulation by food intake in the short-lived vertebrate model *Nothobranchius furzeri*. Our experiments, conducted on male specimens, show that: (a) *HCRT* and OXA and NPY mRNA and protein are localized in neurons of diencephalon and optic tectum, as well as in numerous fibers projecting through the entire neuroaxis, and are colocalized in specific nuclei; (b) in course of aging, *HCRT* and *NPY* expressing neurons are localized also in telencephalon and rhombencephalon; (c) *HCRT* expressing neurons increased slightly in the diencephalic area of old animals and in fasted animals, whereas *NPY* increased sharply; (d) central *HCRT* levels are not regulated neither in course of aging nor by food intake; and (e) central *NPY* levels are augmented in course of aging, and regulated by food intake only in young. These findings represent a great novelty in the study of central orexinergic and NPY-ergic systems in vertebrates', demonstrating an uncommon and unprecedented described regulation of these two orexigenic neuropeptides.

KEYWORDS

aging, food intake, *HCRT*, hypothalamus, NPY, RRID:AB_1566510, RRID:AB_653610, RRID: AB_91545, teleost fish

1 | INTRODUCTION

The role of orexinergic and NPY-ergic systems during vertebrates aging has been widely studied in mammals (Botelho & Cavadas, 2015; Nixon et al., 2015). We propose to employ a non mammalian model species, excellent for brain aging studies (Baumgart et al., 2014; Cellerino, Valenzano, & Reichard, 2016; Cellerino et al., 2016; D'Angelo et al., 2016b): *Nothobranchius furzeri*, considered the shortest-lived vertebrate ever described under laboratory conditions (Valdesalici & Cellerino, 2003). Despite the relatively short lifespan, this fish shows many molecular, cellular, and physiological aging phenotypes that are shared with many other organisms, including humans (Cellerino et al., 2016). Remarkably, the lifespan of *N. furzeri* can be experimentally manipulated by changes in nutrients, drugs, temperature, and social conditions (Terzibasi et al., 2009; Valenzano, Terzibasi, Cattaneo, Domenici, & Cellerino, 2006; Valenzano et al., 2006), as well as genetic modifications (Harel et al., 2015).

Orexin A (OXA) and neuropeptide Y (NPY) are two neuropeptides primarily involved in the regulation of feeding behavior and food intake in all vertebrates (Tachibana & Tsutsui, 2016; Volkoff, 2016). In addition, they orchestrate several physiological processes such as arousal, whole-body energy metabolism, reward seeking, autonomic function, sexual behavior, and ventilatory control (Pedrazzini, 2004; de Lecea & Huerta, 2014). Studies on the molecular regulation of orexin and NPY hypothalamic neurons confirm that they also interact in the control of energy homeostasis (Waterson & Horvath, 2015).

OXA is composed of 33 amino acids with an amino (N)-terminal pyroglutamyl residue, two intra-chain disulphide bonds and carboxy (C)-terminal amidation, produced from a precursor polypeptide, prepro-orexin, also known as hypocretin (*HCRT*), through usual proteolytic processing presumably by prohormone convertases (Sakurai et al., 1998; Tsujino & Sakurai, 2013). OXA has potent effects on the food intake regulation in mammals (Messina et al., 2014) and fish (D'Angelo et al., 2016a; Matsuda et al., 2012a).

NPY was originally isolated from porcine brain extracts (Tatemoto et al., 1982), and is abundantly expressed within the brain. It is one of the most potent orexigenic agents in mammals (Loh et al., 2015) and fish (Ronnestad et al., 2017).

The primary structure of OXA and NPY is conserved among mammalian (Tsujino & Sakurai, 2013) and fish species (Alvarez & Sutcliffe, 2002; Cerdá-Reverter & Larhammar, 2000). Particularly in fish, the genetic and molecular structures, the anatomical localization, and the orexigenic function of OXA and NPY have been abundantly investigated (Cerdá-Reverter & Canosa, 2009; Volkoff, 2016). Neuroanatomical studies have demonstrated a wider distribution of the two neuropeptides, not restricted to the hypothalamus, as in mammals (Ronnestad et al., 2017).

Accumulating evidences suggest that the orexinergic and NPY-ergic systems are involved in aging and lifespan determination. Clear age-related reductions in the orexin system of animal models have been reported in the hypothalamus and other brain regions (Brownell & Conti, 2010; Kessler et al., 2011; Sawai, et al., 2010). Such deregulation affects body weight, food intake, sleep patterns (Nixon et al., 2015), and could contribute to progression of age-related pathologies, such as Parkinson's disease (Wienecke et al., 2012) and

Alzheimer's disease (Slats et al., 2013). Therefore, orexin system represents a promising target for pharmacological therapies (Duarte-Neves, de Almeida, & Cavadas, 2016; Tsuneki et al., 2016). Previous studies suggest that NPY system is also linked to the aging process; however, its role has not been completely clarified. In aged rodents, and in brain samples from individuals with neurodegenerative disease, levels of NPY and NPY receptors decreased in several brain areas (Botelho & Cavadas, 2015). NPY contributes to various age-related mechanisms, for example, NPY induces autophagy in the hypothalamus (Botelho & Cavadas, 2015), and could be critical for the beneficial effects of caloric restriction on aging (Minor et al., 2011).

To better analyze the age-related changes of orexin and NPY in N. furzeri, we conducted experiments in specimens of 5, 12, and 27 weeks old specimens (at sexual maturity, adult, and old stages, respectively), and (a) identified orexin and NPY containing neurons in the diencephalon and midbrain by immunohistochemistry; (b) studied the morphological rearrangement of neuronal expression pattern observed outside diencephalic areas in course of aging by in situ hybridization; (c) assessed that short-term fasting is a metabolic stimulus to trigger neuronal activity; (d) evaluated the unchanged central levels of *HCRT* in course of aging and by food intake; and (e) assessed the overexpression of *NPY*, paralleled by an augmented number of positive neurons, in course of aging and by food intake only in young animals. These findings shed light on new aspects of orexinergic and NPY-ergic systems regulation in the brain of vertebrates during aging.

2 | MATERIALS AND METHODS

2.1 | Animal experiments and fasting

Fish housing and care followed specific standard operating procedures for breeding MZM-0410 strain (median lifespan 40 weeks) (Baumgart et al., 2016). Animals were kept constantly at 26 °C and 12 hr of light-/dark cycles. At the age of 3 weeks post-hatching (wph), young fish were moved to single-housed tanks with low water flow. Salinity was maintained always between 2.5 and 3 mS, and parameters such as pH and mineral content were daily checked to avoid discrepancies between experimental groups. Fish were fed manually and, within 2 hr, uneaten food was removed from the tank to avoid dropping of water parameters. Young fry, from hatching to 20 dph were fed only with *Artemia salina* twice per day. From 21 dph to 34 dph, fish were fed twice a day with *A. salina* and once with *Chironomus plumosus* (bloodworm larvae). This proteic boost is necessary to complete the sexual maturity. At the 35 dph, fish are considered young adults and they were fed just once per day with *C. plumosus* for the rest of their life.

At time points of 5, 12, and 27 wph, animals from the same hatch were divided into experimental and control groups. Experimental groups underwent fasting for 96 hr. Fasted and control animals were euthanized with a bath of 1 g/L tricaine methane-sulfonate (MS-222, Tricaine-S®, in buffered solution, according to AVMA Guidelines for the Euthanasia of Animals, 2013) at room temperature (RT; 26 °C). To avoid effects of circadian rhythms and feeding, animals were always euthanized at 10 a.m., 3 hr after the light phase was began. The whole head and/or brains were dissected and processed according to the

experimental protocols. In addition, the diencephalon (including the inferior lobe of hypothalamus) was microdissected, upon removing telencephalon, mesencephalon, and rhombencephalon. A total number of 84 male specimens were employed: of these 51 were used for RNA extraction and 33 for morphological and western blotting analyses. All experiments were approved by the Italian Competent Authority (authorization number 277/2017-PR).

2.2 | Protein isolation and western blotting

Ribosomal protein S6, a structural component of the ribosome, becomes phosphorylated in neurons activated by a wide range of stimuli, including fasting (Knight et al., 2012), and can be used as a tag to enable the capture of mRNA from activated cells. As the phosphorylation sites on S6 are evolutionarily conserved (Meyuhas, 2008), this approach is used to study a range of species, including those that are not amenable to genetic modification (Knight et al., 2012). We, therefore, evaluated the distribution of pRPS6 in the diencephalic region of *N. furzeri* to confirm that 96 hr of fasting was a sufficient stimulus to activate neurons. Western blotting analysis was conducted to evaluate the expression of endogenous levels of total S6 ribosomal protein independent of phosphorylation (Cell Signaling Technology Cat# 2217, RRID:AB_331355) and phosphorylated ribosomal protein S6 (pRPS6) (Cell Signaling Technology Cat# 4858, RRID:AB_916156) protein expression in the brain of three animals of each experimental group: control animals at 5 and 27 wph, and after 96 hr of fasting at 5 wph. Antibodies are listed in Table 1. The whole brain was dissected on ice and treated with 200 μl of lysis buffer, homogenized by ceramic (zirconium oxide) beads 5× for 1 min in the Tissue Lyser II at 30 Hz. The homogenate was centrifuged at 13.500× g for 15 min and the supernatant was retained. The protein concentration was determined using Bicinchoninic acid (BCA) Protein Assay (Thermo Fisher Scientific Cat# PA1-23227, RRID:AB_558906) and the absorbance spectrum at 560 nm (GloMax®-Multi+Microplate Multimode Reader with Instinct®). Protein aliquots were diluted in loading buffer to have 1 mg/ml of protein and then heated at 95 °C for 10 min. Proteins and molecular weight markers were loaded in 5% stacking and 15% resolving acrylamide gel (30% Acylamide Sigma-Aldrich®, cat. A3699). The gel was casted in Mini-Protean II chambers (Biorad®), filled with the migration buffer, and run 30 min at 80 V first, followed by 1 hr at 120 V. Wet blotting was performed using nitrocellulose membranes (0.2 μm pore size, Biorad®) for 30 min at 100 V, immersed in transfer buffer. To check for success of the transfer, membranes were stained with Ponceau Red. The membranes were blocked with 5% nonfat milk for 1 hr at 4 °C under agitation. The membranes were incubated with the primary antibody, diluted in blocking solution, overnight at 4 °C, under agitation. The membranes were successively incubated with horseradish peroxidase (HRP)-conjugated secondary antibodies, diluted in Tris-buffered saline with Tween (TBS-T), for 1 hr at room temperature (RT) under agitation. The protein was detected, developing by the chemiluminescent system (Clarity™ Western ECL Substrate BioRad, cat.170-5060), after a reaction of 5 min at RT. For reprobing the membranes, Restore™ western blot stripping buffer (Thermo Fisher Scientific Cat# PA5-21059, RRID:AB_11153941) was used 10 min at 26 °C. Western blots were repeated in triplicates and every

experiment was followed by a negative control in which the step of the primary incubation was skipped.

2.3 | Morphological Experiments #1: Immunohistochemistry

The immunohistochemistry (IHC) protocols have been used and described in detail previously (de Girolamo & Lucini, 2011). Experiments were conducted either on frozen or paraffin embedded sections of four adult animals (12 wph), and the used antibodies are listed in Table 1. For paraffin sections, the whole head of adult control animals was dissected and fixed in Bouin's fluid overnight at RT, progressively dehydrated in ascending gradient of ethanol and then transferred to the organic solvent xylene. The brain was embedded in low-melting-temperature paraffin and sectioned in 7 μm thickness. After dewaxing in xylene and rehydrating in progressively diluted alcohols, serial sections were treated with 3% H_2O_2 for 20 min, washed with PBS, and incubated in a humid chamber for 24 hr at 4 °C with each primary antibody diluted with PBS containing 0.2% Triton X-100, 0.1% BSA, and 4% NGS.

Different treatment was carried out depending on the primary antibody in use: incubation with rabbit antibody was followed by incubation with EnVision reagent, containing the secondary antibody (Dako Cat# K4003, RRID:AB_2630375), for 30 min at RT. Sections incubated with antibodies raised in goat were then incubated with anti-goat secondary antibody biotinylated and treated with the avidin–biotin-based peroxidase system (Vectastain ELITE ABC kit, Vector Laboratories, Burlingame, USA, Cat# PK-6100, RRID:AB_2336819). The immunoreactive sites were visualized using a freshly prepared solution of 10 mg of 3,3′-diaminobenzidine tetrahydrochloride (DAB, Sigma-Aldrich, #D5905) in 15 ml of a 0.5 M Tris buffer, pH 7.6, containing 1.5 ml of 0.03% H_2O_2. After a series of alcohol and xylene, slides were sealed with quick-hardening mounting medium (Eukitt, Sigma Aldrich, 03989). Images were analyzed by using Leica DC300 F camera attached to a Leica microscope DM RA2 (Leica Camera AG). Postproduction was analyzed by Adobe Photoshop software.

For the immunofluorescence, after incubation with the primary antisera, the sections were washed several times and incubated with two fluorochrome-conjugated secondary antibodies diluted in 1× PBS for 1 hr at RT, with Alexa 488- (Molecular Probes Cat# A-11055, RRID:AB 142672) and Alexa 568- (Thermo Fisher Scientific Cat# A10042, RRID:AB_2534017) conjugated secondary antibodies (1:500). The slides were thoroughly washed and mounted with glycerol/PBS (1:1). Imaging was performed by a camera attached to a Zeiss ApoTome.2 microscope (Carl Zeiss, Jena, Germany) and postproduction was analyzed by Zeiss Zen 2 Blue and Adobe Photoshop software.

The specificity of each immunohistochemical reaction was checked in repeated trials as follows: (a) substitution of either primary or secondary antibodies by PBS or nonimmune serum and (b) preabsorption of primary antibodies with antigenic peptides (up to 5 mg/ml antiserum in the final dilution). Only for the orexin-A antibody AB3704, the specific inhibition peptide was not available. Sections of mouse hypothalamus were used for positive controls (Cristino et al., 2013).

TABLE 1 Antibodies list used for western blot, immunohistochemistry and immunofluorescence methods

Antibody	Dilution WB	Dilution IHC-IF	Catalogue code	Antigenic peptide
Anti-rabbit neuropeptide Y polyclonal, synthetic peptide within residues 1 to the C-terminus of pig neuropeptide Y	–	1:1,000 P 1:100 FoFr	Abcam Cat# ab30914, RRID: AB_1566510	Pig neuropeptide Y peptide (Abcam Cat# ab32971)
Anti-goat orexin A polyclonal, peptide mapping at the C-terminus of human orexin-A	–	1:500 P 1:10 FoFr	Santa Cruz Biotechnology Cat# sc-8,070, RRID:AB_653610	Santa Cruz Biotechnology Cat# sc-8070p
Anti-rabbit orexin A polyclonal, synthetic peptide corresponding to the C-terminal portion of the bovine orexin-A peptide	–	1:200 P	Millipore Cat# AB3704, RRID: AB_91545	Not available
Anti-rabbit phospho-S6 ribosomal protein monoclonal, monoclonal antibody produced by immunizing animals with a synthetic phosphopeptide corresponding to residues surrounding Ser235 and Ser236 of human ribosomal protein S6	1:2,000	1:1,000 FoFr	Cell Signaling Technology Cat# 4858, RRID:AB_916156	Phospho-S6 ribosomal protein (Ser235/236) blocking peptide (Cell Signaling Technology Cat #1220)
Anti-rabbit S6 ribosomal protein monoclonal, monoclonal antibody produced by immunizing animals with a synthetic peptide corresponding to residues of human S6 ribosomal protein	1:1,000	–	Cell Signaling Technology Cat# 2217, RRID:AB_331355	S6 ribosomal protein blocking peptide (Cell Signaling Technology Cat #1155)
Anti-biotin, HRP-linked	1:1,000	–	Cell Signaling Technology Cat# 7075, RRID:AB_10696897	
Anti-rabbit IgG, HRP-linked	1:2,000	–	Cell Signaling Technology Cat# 7074, RRID:AB_2099233	
Goat anti-rabbit (H + L), Alexa Fluor® 488 conjugate	–	1:1,000 FoFr	Molecular Probes Cat# A-11008, RRID:AB_143165	
Biotinylated rabbit anti-goat (H + L)	–	1:200 P	Vector Laboratories Cat# BA-5000, RRID:AB_2336126	
Donkey anti-goat (H + L), Alexa Fluor® 488 conjugate	–	1:500 FoFr	Molecular Probes Cat# A-11055, RRID:AB_142672	
Donkey anti-rabbit IgG (H + L), Alexa Fluor 568		1:500 FoFr	Thermo Fisher Scientific Cat# A10042, RRID:AB_2534017	

P stands for paraffin and FoFr for frozen sections.

2.4 | Morphological Experiments #2: In situ hybridization

Dissected brains of the following were used: 4 adult animals (12 wph, control), 4 animals (5 wph, control), 4 animals (27 wph, control), 4 animals (5 wph, fasted animals - FA), and 4 animals (27 wph, FA).

Brains were dissected and fixed in 4% RNAse-free paraformaldehyde at 4 °C for 24 hr, and then treated with 20% sucrose for 12 hr and 30% sucrose overnight at 4 °C. They were embedded in cryo-embedding-medium (O.C.T. tissue tek Richard-Allan Scientific™ Neg-50™, #6502) and kept at −80 °C. Cryostat sectioning was performed in coronal orientation of 8 μm thickness. To generate the probes, a pool of RNA, extracted from MZM-0410 brain, was used to synthesize cDNA as template for the following reactions. Oligonucleotide primers were designed using Primer3 software (*HCRT*: _fw ATC AGA TGA CTG CCC TCC AT; _rv GGT AAT ACG ACT CAC TAT AGG AGT TCA CTG CTC CCC AGT TG. *NPY*: _fw GAA AGC CAC TGG GAC AAA TC; _rv GGT AAT ACG ACT CAC TAT AGG GCC CCA TCT CCG TTT TCT AT). Each reverse primer contained a T7-promotor sequence to allow direct in vitro transcription. The primers were dissolved to a final concentration of 10 pM. A standard PCR was run to amplify the target region, using an annealing temperature of 60 °C. An analytical

1% agarose gel was casted to check for the expected length of the amplicon. Preparative 1% agarose gel was used to cut out the band of interest and DNA was cleaned by use of Illustra GFX PCR DNA and Gel Band Purification Kit (GE Healthcare Life Science, 28-9034-70), following the manufacture protocol. A total of 300 ng of the products were sequenced and aligned by the Molecular Evolutionary Genetics Analysis (MEGA6) software to validate the expected sequence of the amplicon (Table 2).

RNA labeling with Digoxigenin-11-dUTP by in vitro transcription with T7 polymerase was carried out with DIG RNA labeling mix (Roche, 11277073910) following the manufacturer's protocol, using 200 ng of PCR product as template. After lithium-chloride precipitation, the concentration of RNA was quantified with a NanoDrop 1000 (PeqLab, Erlangen, Germany). Dot blot was performed to guarantee the proper DIG incorporation into the newly synthesized transcript according to the protocol by Zimmerman et al. (2013). In addition, to verify the length of the transcript, it was checked on a denaturing 4% Urea-TBE polyacrylamide gel. The protocol used for the ISH on cryo-sections was performed according to Tozzini et al., (2012), and the hybridization temperature was 55 °C (temperature set according to GC content). Staining of the probes were developed with Fast Red

TABLE 2 Nucleotides sequences

HCRT (404 nts)
ATCAGATGACTGCCCTCCATAAAAGCCTGAAGATGACGTGGAGCCCCTCCAAGATCCAGAAAGCTGCTAGGATGGACACAACGCACAAGAAAGCCCTGGTGTTCGTTTT GATGTTGCTGCTGTCTCAGCTGGATTGTAACGCCCAAATTGTGTCTGAGTGCTGCAGACAGCCTCCTCACTCCTGCCGCCTCTATGTCTTACTGTGCCGTTCTGG CAGCAATAGCATGGGGGGAACAATTGTAGAAGATGCAGCTGCTGGGATCCTCACGCTGGGTAAACGGGACGAGAATGAGTATCGCTTGCAGAGCCGACTCCACCAGC TTCTTCACAGCTCCAGGAACCAAGCAGCAGGGATCCTGACGATGGGGAGGAGGACCACTGGGCCAACTGGGGAGCAGTGAACT.

NPY (513 nts)
ATCAGATGACTGCCCTCCATAAAAGCCTGAAGATGACGTGGAGCCCCTCCAAGATCCAGAAAGCTGCTAGGATGGACACAACGCACAAGAAAGCCCTGGTGTTCGTTTTGAT GTTGCTGCTGTCTCAGCTGGATTGTAACGCCCAAATTGTGTCTGAGTGCTGCAGACAGCCTCCTCACTCCTGCCGCCTCTATGTCTTACTGTGCCGTTCTGGCAGCA ATAGCATGGGGGGAACAATTGTAGAAGATGCAGCTGCTGGGATCCTCACGCTGGGTAAACGGGACGAGAATGAGTATCGCTTGCAGAGCCGACTCCACCA GCTTCTTCACAGCTCCAGGAACCAAGCAGCAGGGATCCTGACGATGGGGAGGAGGACCACTGGGCCAACTGGGGAGCAGTGAACT.

solution (Roche Tablets; 1 in 2 ml Tris–HCl 0.1 M, pH = 8.2). Nuclei were stained with DAPI mounting medium (IBSC, cat # AR-6501-01) before sealing with coverslips.

2.5 | Morphological Experiments #3: Combined in situ hybridization and immunofluorescence

To verify that *NPY* expressing neurons were activated by fasting stimulus, sections were processed for immunostaining against pRPS6 just after hybridization with the *NPY* probe. After Fast Red solution, sections were washed in PBS, incubated first with normal goat serum blocking solution (NGS, Thermo Fisher Scientific Cat# 01-6201, RRID: AB_2532945) for 2 hr at RT, and then with pRPS6 primary antibody overnight at 4 °C. After washing in RNAse free PBS, sections were incubated with fluorochrome-conjugated secondary antibody for 1 hr at RT and nuclei were stained with DAPI mounting medium before sealing with coverslips. Imaging acquisition and analysis was performed as described in the immunofluorescence. Micrographs were saved in TIFF format and adjusted for light and contrast before cell counting. Cell count was carried out manually by using an open source image-processing program (ImageJ). Only cells with distinguishable nucleus were taking into account. Autofluorescent erythrocytes were excluded from the counting. Erythrocytes could be unambiguously identified based on typical nucleated morphology (nucleus diameter ≤ 0.09 pixels, at 20×). Thus, all positive cells with nucleus diameter ≤ 0.09 pixels (at 20×) were not considered, in order to avoid inclusion of erythrocytes into the count. The graphical analysis was produced by GraphPad Prism and Adobe Illustrator.

2.6 | HCRT and NPY mRNAs expression in hypothalamus and whole brain of *N. furzeri*

To verify whether levels of *HCRT* and *NPY* are altered by fasting, the analysis of their mRNAs expression was carried out in the dissected hypothalamus of young (5 wph) and old (27 wph) *N. furzeri* in fasted or fed state (*n* = 5 per group, *n* = 20 in total).

We then analyzed the expression levels of *HCRT* and *NPY* mRNAs in the whole brain of in total 31 animals at 5 wph (*n* = 6), 12 wph (*n* = 6), and 27 wph (*n* = 19), because the neuroanatomical experiments revealed a wide distribution throughout the neuroaxis. The whole brain was dissected on ice and RNA was extracted as described in Baumgart et al. (2014). Real-time PCR was performed with the CFX384 (Biorad) and the Quantitect PCR system (Qiagen). Steps were processed as recommended by the manufacturer. Forward and reverse primers were always located

in two different exons (HCRT: _fw TGA CTG CCC TCC ATA AAA GC; _rv GCT GAG ACA GCA GCA ACA TC. NPY: _fw CAG CCC TGA GAC ACT ACA TCA; _rv CTG CTC TCC TTC AGC AGC A.). A cDNA pool was serially diluted (from 80 to 2.5 ng per reaction) and used to create standard as well as melting curves and to calculate amplification efficiencies for each primer pair prior use for quantification. All reactions were performed in triplicates and negative (water) as well as genomic (without reverse transcriptase) controls were always included. Fold changes described the difference in expression level between young and old age animals normalized to TATA-box binding protein (TBP: _fw CGG TTG GAG GGT TTA GTC CT; _rv GCA AGA CGA TTC TGG GTT TG). TBP was chosen as normalizer, since our RNA-seq data (Baumgart et al., 2014) show no significant aging associated expression changes in the brain of the analyzed strain between 5 and 27 wph. Primers were designed based on the *N. furzeri* transcriptome browser (https://gen100. imb-jena.de/EST2UNI/nfintb/). Expression levels were calculated by delta CT method relative to TBP, and fold changes are calculated relative to 5 wph controls. Statistical analysis of real-time data was done by unpaired two-tailed *t* test and ANOVA posttest for linear trend (GraphPad Prism 7). We have corrected all *p*-values for multiple comparisons using Bonferroni's method.

3 | RESULTS

3.1 | Localization of HCRT and OXA, NPY mRNA and protein in the diencephalon/midbrain of adult male animals

To study the neuronal orexinergic and NPY-ergic systems in more detail, we performed IHC with antibodies raised against mammalian OXA and NPY, whose conservation degree is shown in Figure 1, and in situ hybridization to evaluate the localization of HCRT and NPY mRNAs expressing neurons. The experiments were conducted on adult animals (12 wph) kept under standard conditions, suppressed before the morning feeding. The results are semiquantitatively summarized in Table 3. Drawings of the brain of *N. furzeri* (D'Angelo, 2013) recapitulate schematically the neuroanatomical distribution of orexin and NPY in the diencephalon/midbrain (Figures 2 and 3).

OXA immunoreactive and HCRT mRNA expressing neurons were detected in: ventral telencephalon, magnocellular part of the preoptic nucleus, cortical nucleus, central pretectal nucleus, ventral accessory optic nucleus, anterior and ventro-medial and lateral thalamic nuclei, and in proximity of the ventricle, lateral, anterior and caudal part of

FIGURE 1   (a) *NPY* and *HCRT* intron/exon gene structure of *N. furzeri* and alignment of transcripts from other fish species (downloaded and modified from http://nfingb.leibniz-fli.de/, transcript information for the other fish species can be found at http://www.ensembl.org/). (b) NPY protein sequence alignments in different vertebrate species: *N. furzeri*; *Oryzias latipes* (medaka); *Carassius auratus* (goldfish) and *Mus musculus* (mouse). Asterisks mark conserved amino acids (alignment was done with Clustal Omega http://www.ebi.ac.uk/Tools/msa/clustalo/).
(c) HCRT/Prepro-orexin protein sequence alignments in different vertebrate species: *N. furzeri*; *Oryzias latipes* (medaka); *Carassius auratus* (goldfish) and *Mus musculus* (mouse). Asterisks mark conserved amino acids (alignment was done with Clustal omega http://www.ebi.ac.uk/Tools/msa/clustalo/) [Color figure can be viewed at wileyonlinelibrary.com]

TABLE 3 Semiquantitative analysis of NPY protein and mRNA, OXA, and HCRT distribution in the diencephalic regions of adult (12 wph) *N. furzeri*

Neuroendocrine regions	NPY Protein Neurons	NPY Protein Fibers	NPY mRNA Neurons	OXA Protein Neurons	OXA Protein Fibers	HCRT mRNA Neurons
Telencephalon						
Central zone of dorsal telencephalon (Dc)		++			+++	
Dorso-lateral zone of dorsal telencephalon (Dld)		++			++	
Latero-lateral zone of dorsal telencephalon (Dll)		++			++	
Ventro-lateral zone of dorsal telencephalon (Dlv)		++			+++	
Medial zone of dorsal telencephalon (Dm)		++			++	
Ventral telencephalon (Vv)		++	++	++	++	++
Ventro-lateral telencephalon (Vl)		++			++	
Preoptic area						
Suprachiasmatic nucleus (SC)		++	++		++	
Preoptic nucleus, parvocellular part (PPp)			++		++	
Preoptic nucleus, magnocellular part (PM)			++	++	+	++
Tuberal hypothalamus						
Dorsal hypothalamus (Hd)	+	++	++	++	+++	
Ventral hypothalamus (Hv)	++	++	++		+++	
Caudal hypothalamus (Hc)			++			
Lateral hypothalamus (Hl)			++	+	++	
Anterior tuberal nucleus (TNa)	+		++			
Posterior tuberal nucleus (TNp)	+					
Periventricular nucleus of posterior tuberculum (TPp)	++	+	+			+
Preglomerular nucleus (PG)		++	+		++	+
Glomerular nucleus (NG)	+++	++	+	+++	+	+
Hypothalamic recess (rec)	++	+	++	++	+++	+
Nucleus of posterior recess (NRP)			++			++
Inferior lobe of hypothalamus (DIL)	+++	++	++	+++	++	++
Posterior tubercle						
Paraventricular organ (PVO)	++		+	++	++	+
Thalamus						
Ventro-medial thalamic nucleus (VM)			++	++		+
Ventro-lateral thalamic nucleus (VL)	++			++		+
Central pretectal nucleus (CPN)	+	++	++	+	++	
Dorsal periventricular pretectal nucleus (PPd)			++			
Superficial pretectal nucleus (SPN)			++			
Cortical nucleus (NC)	+++	++		+++		++
Ventral accessory optic nucleus (VAO)	++			++	++	++

+ = few; ++ = moderately dense; +++ = very dense.

dorsal hypothalamus, paraventricular organ, inferior lobe of the hypothalamus (Figure 4a,e,e₁,d) and hypothalamic recess, and in addition in cells of periventricular gray zone, lining the deep white and gray zone. OXA immunoreactive fibers were widespread and projecting throughout the whole brain (Figure 4a,b).

NPY immunoreactive and NPY mRNA expressing neurons were seen in: ventro-lateral (Figure 5a,b) part of the telencephalon, cortical nucleus (Figure 5c), ventral accessory optic nucleus (Figure 5c), ventro-lateral thalamic nucleus (Figure 5e,f), along the margin of the ventral hypothalamus (Figure 5c,d,d₁), in proximity of the ventricle (Figure 5c,d), dorsal part of hypothalamus (Figure 5e,f), central pretectal nucleus, periventricular nucleus of posterior tuberculum, anterior and posterior parts of tuberal nucleus; medial and lateral parts of inferior lobe of hypothalamus (Figure 5g,h,h₁), and in addition in cells of periventricular gray zone (Figure 5e,f₁). Moreover, NPY immunopositive fibers were detected in the whole telencephalon (Figure 5a), in pretectal nucleus, around periventricular nucleus of posterior tuberculum; in anterior and posterior parts of tuberal nucleus; in central zone of the optic tectum (Figure 5c), and widely distributed along the neuroaxis.

We also conducted experiments of double immunofluorescence to evaluate if OXA and NPY are codistributed in neurons. Colocalization was detected in some neurons of the cortical nucleus (Figure 6a), ventro-lateral thalamic nucleus and dorsal hypothalamus (Figure 6b,c), and inferior lobe of hypothalamus (Figure 6d).
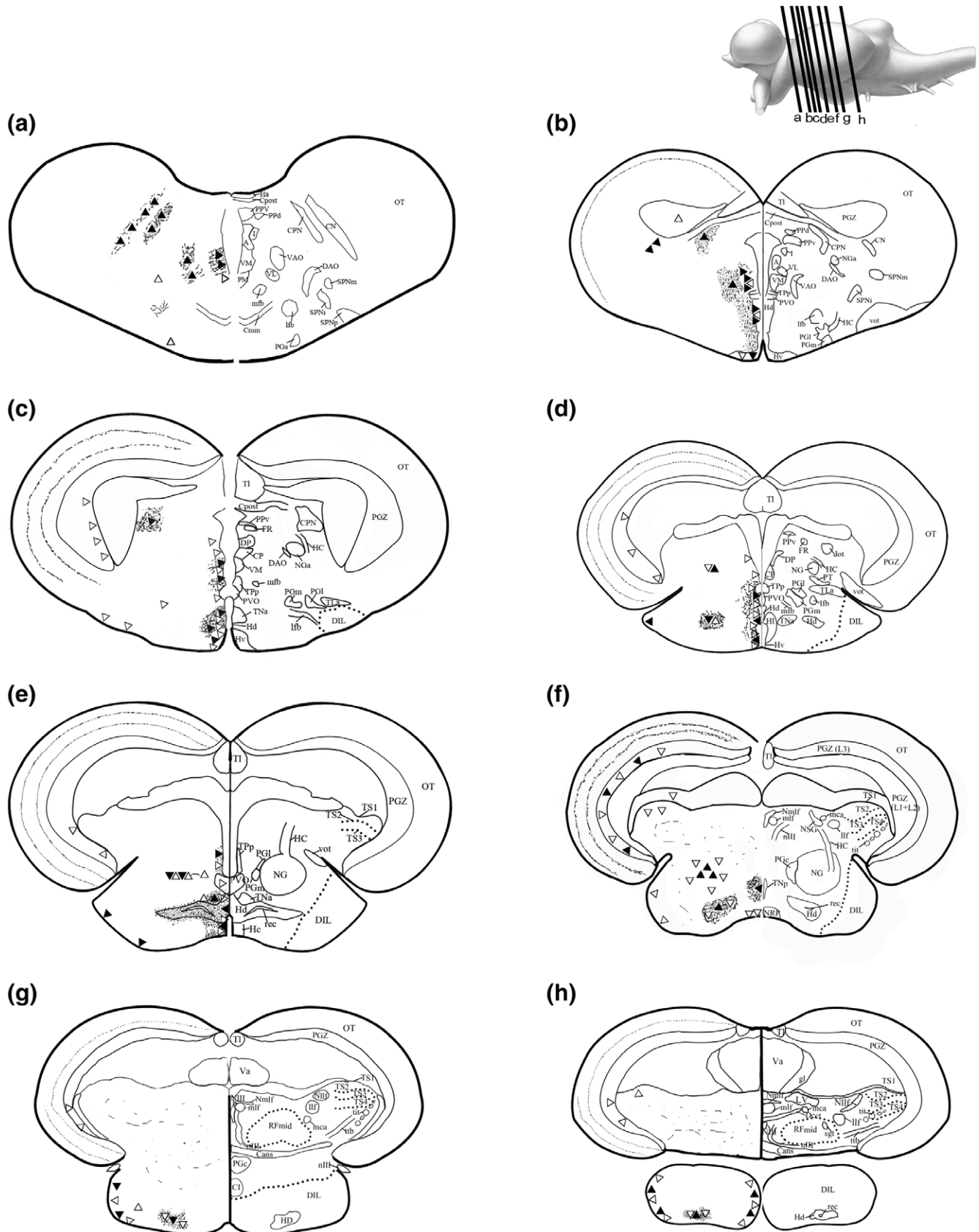
FIGURE 2 Schematic drawings of transversal sections of *N. furzeri* brain (D'Angelo, 2013), specifically referred to diencephalon/midbrain. Each section documents on the right side the abbreviated names of nuclei, and on the left side the pattern of *HCRT* expression in neurons (empty triangles), and OXA distribution in neurons (black triangles) and fibers (black dots)

FIGURE 3 Schematic drawings of transversal sections of *N. furzeri* brain (D'Angelo, 2013), specifically referred to diencephalon/midbrain. Each section documents on the right side the abbreviated names of nuclei, and on the left side the pattern of NPY mRNA expression in neurons (empty triangles), and NPY distribution in neurons (black triangles) and fibers (black dots)
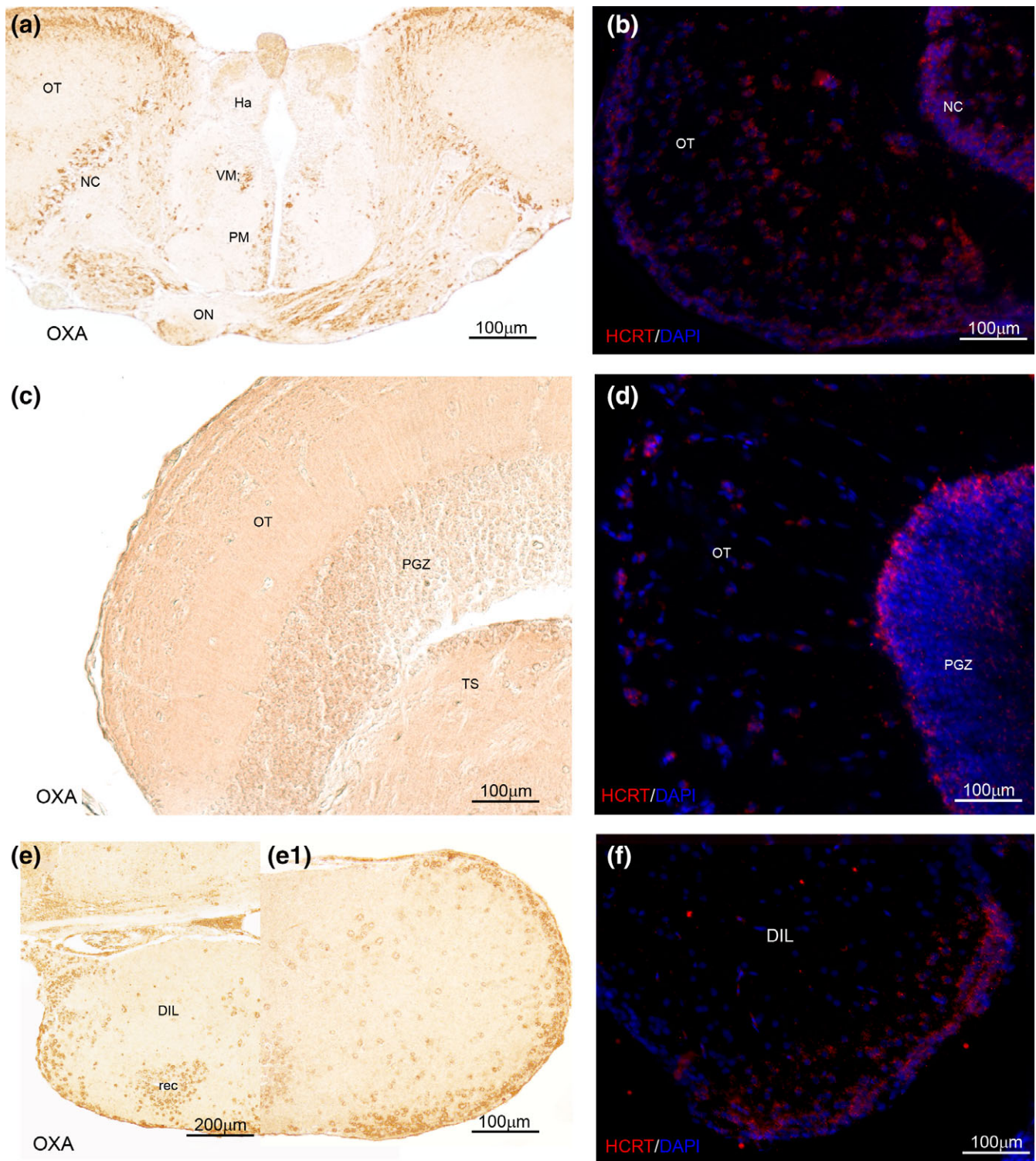
FIGURE 4 Transversal section of OXA immunohistochemical distribution and *HCRT* in situ hybridization in the diencephalon and midbrain of *N. furzeri*. (a) Immunoreactivity (IR) in neurons of PM, CN, VM, and widespread positive fibers of ON projecting toward OT. (b) *HCRT* expressing neurons in the anterior part of OT and in neurons of NC. (c) IR in fibers of the most superficial layers of OT and in some positive neurons of PGZ. (d) *HCRT* expressing neurons in the PGZ of OT, more numerous at the margin between PGZ and the DWGZ of OT. (e) IR in neurons of DIL. **(e₁)** High magnification of neurons in (e). (f) *HCRT* expressing neurons in the DIL [Color figure can be viewed at wileyonlinelibrary.com]

3.2 | HCRT and NPY mRNAs expressing neurons in the diencephalon upon aging and fasting

After describing the neuroanatomical localization of OXA immunoreactive and HCRT mRNA expressing neurons, NPY immunoreactive and HCRT mRNA expressing neurons, we studied the pattern of expression of *HCRT* and *NPY* mRNAs in the hypothalamic areas of *N. furzeri*, at 5 and 27 wph, and upon 96 hr of fasting in subjects at 5 and 27 wph.

HCRT mRNA signal was seen in the dorsal hypothalamus (Figure 7a–d) in all four analyzed conditions. In old control animals, *HCRT* mRNA signal was also seen in the ventro-medial thalamic nucleus; central pretectal
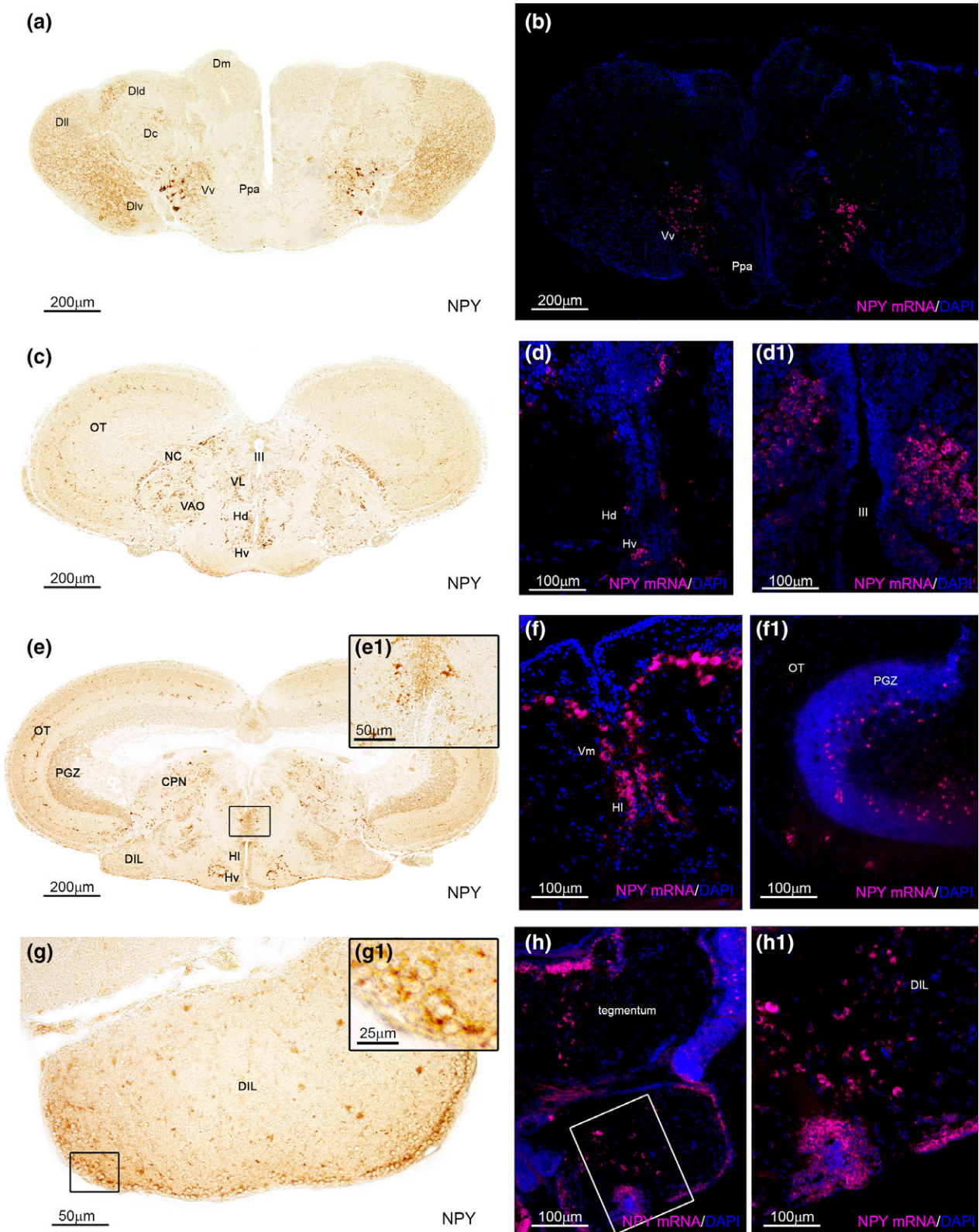
FIGURE 5 Transversal section of NPY immunohistochemical distribution and *NPY mRNA* in situ hybridization in the diencephalon and midbrain of *N. furzeri*. (a) Overview of the caudal telencephalon, showing IR in neurons of Vv and in widespread fibers over the posterior portions of telencephalic hemispheres (Vl, Dld, Dll, Dm, Dc), PPa, and ON. (b) Overview of the caudal telencephalon, showing *NPY* mRNA expressing neurons in Vv. (c) IR in neurons of NC, VAO, VL, Hd, Hv, and positive fibers in the OT and ON. (d) *NPY* mRNA expressing neurons in Hd and Hv. (d$_1$) High magnification of NPY mRNA expressing cells along the ventricle. (e) Overview of diencephalon/midbrain, showing IR in neurons of VL, Hl, Hv, DIL and in some cells of PGZ, and widespread fibers in the caudal part of diencephalon and OT. (e$_1$) High magnification of IR in neurons and fibers of VL. (f) *NPY* mRNA expressing neurons in VL and Hl. (f$_1$) *NPY* mRNA expressing cells of PGZ. (g) IR in neurons of DIL. (g$_1$) High magnification of neurons in the rectangle of (g). (h) *NPY mRNA* expressing neurons in the midbrain tegmentum, in cells at the margin between OT and midbrain tegmentum, and in neurons of rec and DIL. (h$_1$) High magnification of rectangle in (h) [Color figure can be viewed at wileyonlinelibrary.com]
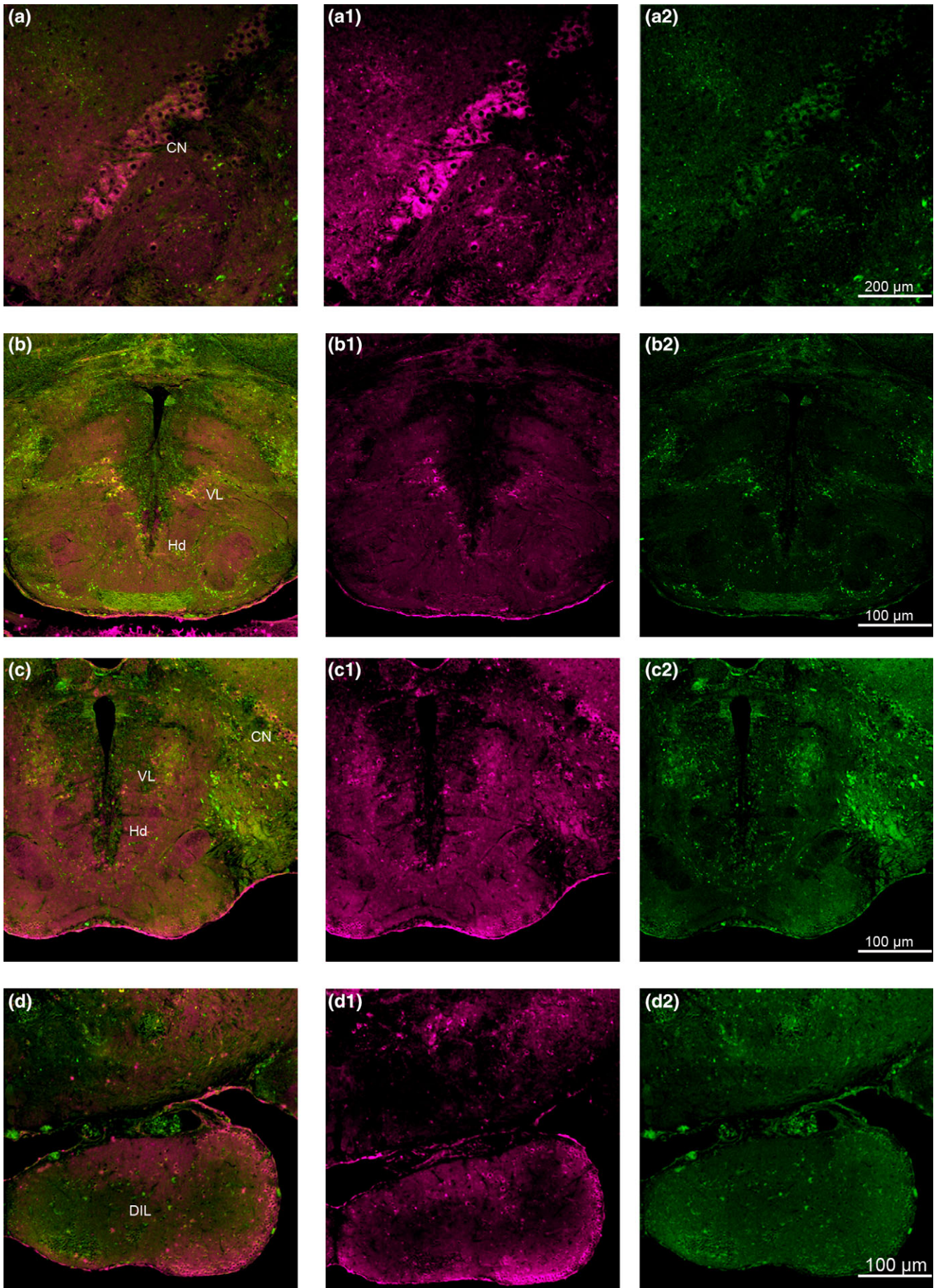
nucleus (Figure 7b); inferior lobe of hypothalamus. Upon fasting, in young animals *HCRT* mRNA probe signal increased sharply, revealing intense positivity in the diencephalon (Figure 7c).

NPY mRNA signal was seen in the ventro-lateral and ventro-medial thalamic nuclei in all four analyzed conditions (Figure 7e–h). In control animals at 5 wph, *NPY* mRNA positive neurons were detected in suprachiasmatic nucleus, parvocellular, and magnocellular part of preoptic nucleus; preglomerular nucleus; anterior tuberal nucleus (Figure 7e). In control animals at 5 wph, NPY mRNA was observed in: paraventricular organ (Figure 7f); nucleus of posterior recess; around the glomerular nucleus; dorsal (Figure 7f), ventral (Figure 7f), lateral (Figure 7g) and caudal hypothalamus; inferior lobe of hypothalamus. In FA at 5 wph, NPY mRNA expressing neurons were seen in the dorsal, ventral (Figure 7g), lateral (Figure 7g), and caudal hypothalamus; inferior lobe of hypothalamus, in proximity of the ventricle (Figure 6g). In FA at 27 wph, intense staining was seen in the whole hypothalamic region, and superficial and central pretectal nuclei (Figure 6h). Notably, either in course of aging and upon fasting in young animals, *NPY* mRNA expressing neurons were numerous. We, therefore, investigated the localization of nuclei responsible for this overexpression by studying also the anatomical distribution of the neuronal activity marker pRPS6 (Jennings et al., 2013) throughout these regions. In old animals, the number of positive pRPS6 neurons decreased significantly in old control (Figure 7f), and very few *NPY* positive neurons were coexpressed with pRPS6 (Figure 7f). As expected, 96 hr of fasting determined a neuronal activation, displayed by the increased number of pRPS6 positive neurons in the brain of young (Figure 7g) but not old animals (Figure 7h).

3.3 | HCRT and NPY mRNAs expressing neurons in non diencephalic regions of old *N. furzeri*

The wider distribution of *NPY* in the diencephalic region of aged animals prompted us to question whether *NPY* could be also expressed outside diencephalon. *HCRT* positive neurons were seen in the rostral part of dorsal telencephalon (Figure 8a) and dorso-medial, dorso-lateral and dorso-ventral portions of the telencephalic hemispheres (Figure 8b) in the periventricular gray zone of the optic tectum. *NPY* mRNAs synthesizing neurons were observed in the dorsal accessory optic nucleus (Figure 8c), in the periventricular gray zone of the optic tectum (Figure 8d) and in the semicircular torus.

3.4 | Age related changes of HCRT and NPY

After having described the distribution of *HCRT* and *NPY* in the young and old *N. furzeri* brain, we analyzed age-dependent regulation of these peptides by qPCR in whole brains. For this aim, we compared the three selected time-points 5 wph (young, sexual maturity), 12 wph (adult), and 27 wph (old) with previous RNA-seq results

obtained at the same age steps in different animals (Baumgart et al., 2014). *HCRT* expression was not found by qPCR and RNA-seq to be statistically significant regulated reduced in the brain of old subjects (Figure 9a,b) to 50% of the young level while *HRCT* expression of the adult animals was reduced to 36% of the young levels (qPCR: $F_{(1,29)} = 5.69$, $p = 0.0952$; RNA-seq: $F(1,12) = 3.136$, $p = 0.408$, ANOVA posttest for linear trend with Bonferroni's correction).

NPY expression levels increased progressively from young, to adult and old animals (Figure 9c). Indeed, the mean expression level in the old subjects was 1.78 times higher than in the young subjects. The expression level of the adult fish was 1.31 times higher than in the young. The expression level of the adult fish was 0.73 times lower than the old ($F(1,28) = 27.62$, $p = 0.0004$, ANOVA posttest for linear trend with Bonferroni's correction). *NPY* expression levels were much higher than *HCRT* (~40 reads per kilobase of transcript, per million [RPKM] in young animals) and age-dependent upregulation of *NPY* was detected also by RNA-seq ($F(1,12)$, $p = 0.0012$, ANOVA posttest for linear trend with Bonferroni's correction) (Figure 9d).

3.5 | Age-related regulation of HCRT and NPY by food intake

In order to test whether these orexigenic peptides in *N. furzeri* are regulated by food intake in young (5 wph) and old (27 wph) specimens, we carried out experiments of fasting, the most used paradigm to evaluate energy homeostasis regulatory process. We, therefore, compared the expression of *HCRT* and *NPY* in control animals and FA. Since both peptides are expressed also outside of the hypothalamus, we performed qPCR on dissected diencephalon. A statistically significant upregulation of *NPY*, but not of *HCRT*, was detected only in young animals (Figure 10a,b) *HCRT*: $t(8) = 1.342$, $p = 1.299$; *NPY*: $t(8) = 4.278$, $p = 0.0162$ two-tailed, unpaired t test with Bonferroni's correction).

We then identified a number of diencephalic nuclei, where expression of *NPY* could be detected only in old subjects and investigated the localization of nuclei responsible for this *NPY* upregulation by counting cells expressing *NPY* or expressing the neuronal activity marker pRPS6 (Figure 10c) (Jennings et al., 2013). In young FA (Figure 10d), a prominent upregulation of *NPY* was detected in 17 diencephalic nuclei out of 19, namely in the DIL, dorsal, ventral, caudal hypothalamus, and several additional nuclei (SC, PPp, SPN, CN, CPN, PG, NG, rec, PVO, A). In old animals (Figure 10e), *NPY* upregulation was observed in eight nuclei, namely in the DIL, dorsal, ventral, caudal hypothalamus, and other nuclei (PPp, PPd, VAO, TP, rec, PVO). Remarkably, pRPS6 immunoreactive cells were scarcely detectable in old specimens, upon fasting, with the exception of very few positive neurons in the SC and DIL (Figure 10e). However, western blot analysis (Figure 10c) on total brain extracts revealed brain-wide upregulation of pRPS6.

FIGURE 6 Double immunofluorescence of OXA (red) and NPY (green) in the diencephalon/midbrain of *N. furzeri*. (a) Codistribution in neurons of NC. (a_1,a_2) Single immunostaining of OXA and NPY. (b) Copresence in some neurons of Hd and VL and in some fibers of ON. (b_1,b_2) Single immunostaining of OXA and NPY. (c) Colocalization in some neurons of VL, Hd and NC. (b_1,b_2) Single immunostaining of OXA and NPY. (d) Codistribution in neurons displaced in the central part and in the peripheral area of DIL. (d_1,d_2) Single immunostaining of OXA and NPY [Color figure can be viewed at wileyonlinelibrary.com]
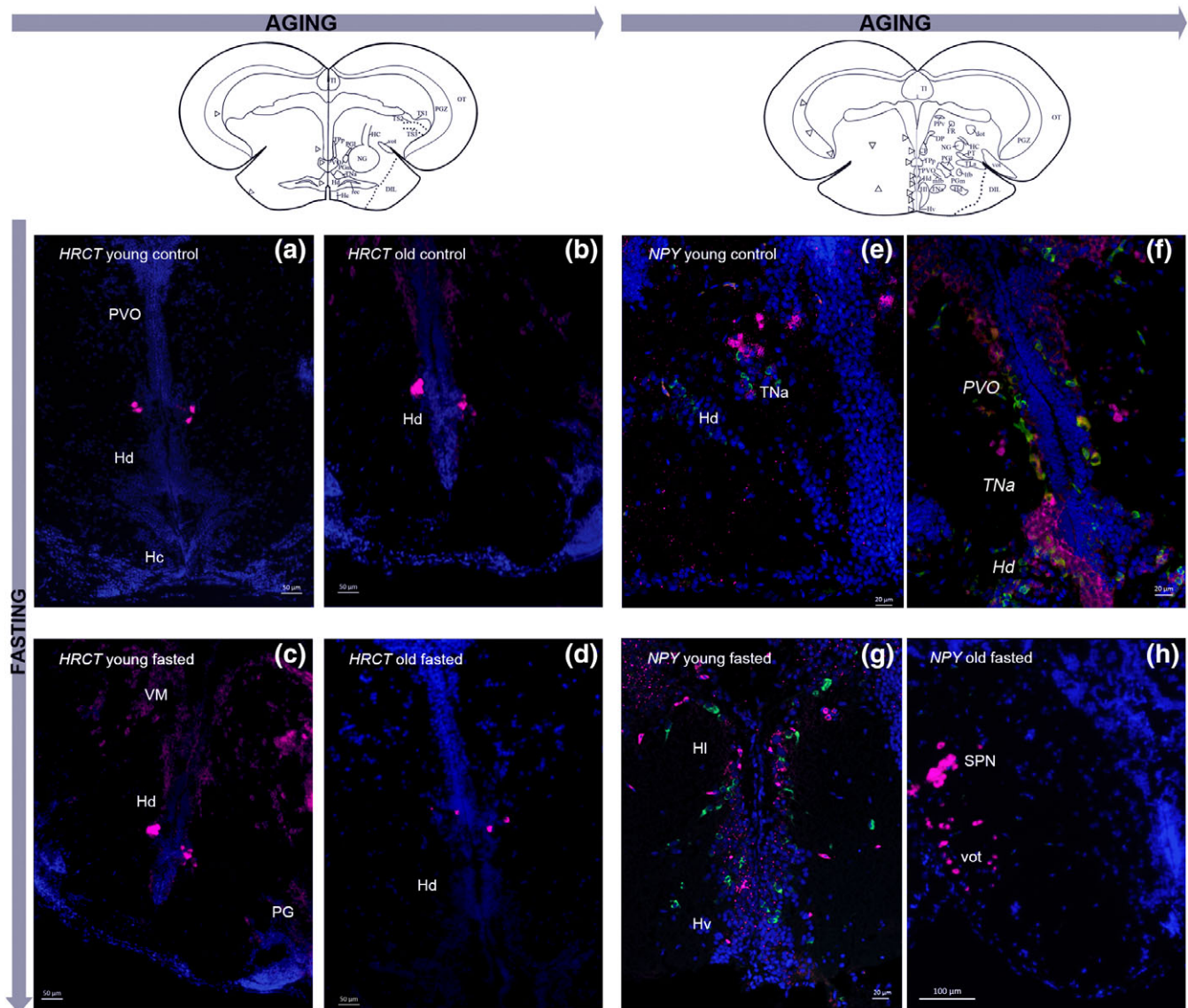
FIGURE 7 HCRT and colocalization of NPY mRNAs/pRPS6 expressing neurons in the diencephalon of *N. furzeri*, upon aging and fasting. On the top schematic drawing depicting the diencephalon/midrain where the probes signal was intensely detected. *HCRT mRNA in control animals:* (a) At 5 wph, few intensely stained neurons in Hd; (b) At 27 wph, markedly few stained neurons in Hd, and slight signal probes in numerous neurons in the most caudal diencephalic nuclei (arrow); *HCRT mRNA in Fa.* (c) At 5 wph, markedly few stained neurons in Hd, in numerous neurons in VM and PG, and signal probe over the most caudal diencephalic region; (d) At 27 wph, few stained neurons in Hd. *NPY mRNA(red)/pRPS6(green) protein (used as marker of activated neurons) in control animals.* (e) At 5 wph, few NPY mRNA neurons in the diencephalic region, and activated neurons in Hd and TNa; (f) At 27 wph, numerous NPY mRNA positive neurons, in PVO, Hd, Hl and Hv. Very few activated neurons in PVO and Hd, and only 2–3 costained neurons in Hd; *NPY mRNA(red)/pRPS6(green) protein (used as marker of activated neurons) in FA:* (g) At 5 wph, NPY mRNA and pRPS6 in several neurons of the hypothalamus (Hv, Hl), without colocalization; (h) At 27 wph, NPY mRNA labeling in neurons of SPN and around vot. Any immunostaining was detected against pRPS6. Nuclei are counterstained with DAPI [Color figure can be viewed at wileyonlinelibrary.com]

4 | DISCUSSION

4.1 | Neuroanatomical organization of orexinergic and NPY-ergic neurons

Orexin and NPY containing neurons were widely distributed in the diencephalon/midbrain of adult *N. furzeri*, kept under standard conditions. OXA and NPY positive neuronal projections were observed throughout the brain, from telencephalon to brainstem, as reported in the brain of different vertebrate species (Peyron et al., 1998; Shibahara et al., 1999; Kaslin et al., 2004; Huesa et al., 2005; Nakamachi et al., 2006;

Nixon & Smale, 2007; Kojima et al., 2009; Matsuda et al., 2012a; Matsuda, et al., 2012b; Miranda et al., 2013; Volkoff, 2016). OXA neuronal projections were not observed in the cerebellum, as documented in rat (Nambu et al., 1999). Remarkably, neurons expressing *HCRT* and *NPY* mRNAs were mainly localized in the hypothalamic areas, and along the third ventricle. Overall, in *N. furzeri*, the distribution of OXA- and NPY-ir cell bodies matched that of *HCRT* and *NPY*-mRNAs expressing cells. Our morphological analyses are in agreement to what has been documented in several fish species (Volkoff, 2016), and different to mammals (de Lecea et al., 1998; Sakurai et al., 1998). Of relevance, *HCRT* expressing neurons in zebrafish (Kaslin et al., 2004)
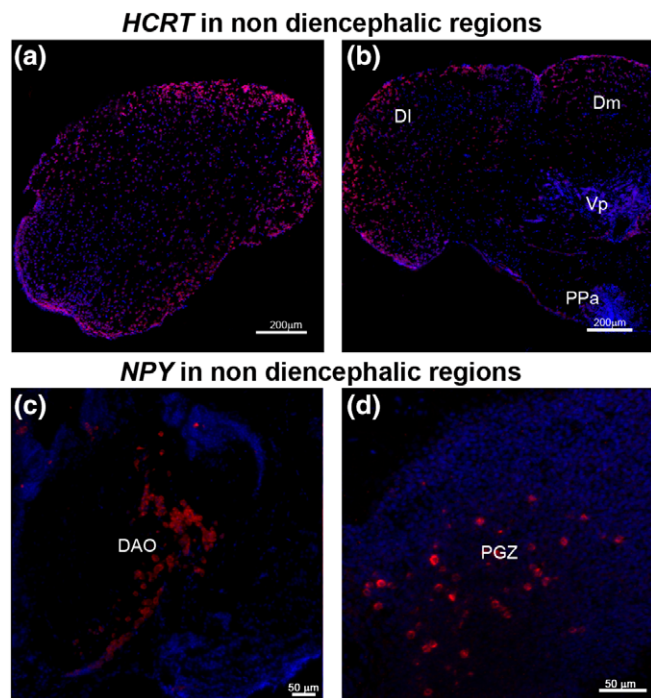
FIGURE 8 *HCRT* and *NPY* mRNAs expressing neurons outside diencephalon/midbrain in animals at 27 wph. Widespread expression of *HCRT mRNA*: (a) in the rostral part of dorsal telencephalon; (b) in Dl and Dm of telencephalon. *NPY mRNA* signal (c) in neurons of DAO; (d) in cells of the PGZ. Nuclei are counterstained with DAPI [Color figure can be viewed at wileyonlinelibrary.com]

FIGURE 9 Age related changes of *HCRT* and *NPY* in the whole brain of *N. furzeri*, in subjects at 5 wph (young, sexual maturity), 12 wph (adult) and 27 wph (old). (a) Age-dependent regulation of *HCRT* levels by qPCR. *HCRT* expression is not statistically significant regulated in the brain of adult and old animals ($F(1,29) = 5.69$, $p = 0.0952$ ANOVA posttest for linear trend with Bonferroni's correction). (b) Age-dependent regulation of *HCRT* levels by RNA-seq. *HCRT* expression is not statistically significant regulated in the brain of adult and old animals ($F(1,12) = 3.136$, $p = 0.408$). (c) Age-dependent regulation of *NPY* levels by qPCR. *NPY* expression levels increased progressively from young, to adult and old animals ($F(1,28) = 27.62$, $p = 0.0004$, ANOVA posttest for linear trend with Bonferroni's correction). (d) Age-dependent upregulation of *NPY* levels by RNA-seq. *NPY* expression levels increased progressively from young, to adult and old animals ($F(1,12)$, $p = 0.0012$, ANOVA posttest for linear trend with Bonferroni´s correction). Fold changes were calculated for each animal relative to the mean expression level of the young controls. TBP was used as housekeeping gene

are restricted to few hypothalamic nuclei. Overall, the wide distribution of positive OXA and NPY projections in the brain of *N. furzeri* prompted us to hypothesize that the two neuropeptides may orchestrate multiple functions, including those in relation with visceral organs (Brothers & Wahlestedt, 2010; Inutsuka & Yamanaka, 2013). For example, the evidence of OXA immunoreactivity reported in the digestive system of different teleostean species (D'Angelo et al., 2016a; Volkoff, 2016) suggests a signaling between central hypothalamic nuclei and peripheral enteroendocrine cells, and discoveries of such networks and messengers provide new biological insights on how to manipulate appetite-satiety pathways and thus their involvement in the regulation of energy homeostasis. More interestingly, both orexinergic and NPY-ergic neurons were located in proximity of the ventricle where the blood brain barrier is more permissive. Indeed, these neurons are more sensitive to peripheral chemical (e.g., glucose) or endocrine (e.g., gastrointestinal hormones) factors circulating in the blood (Volkoff, 2016). These observations suggest the involvement of orexin and NPY neurons in the circuitry of appetite control.

Our results displayed that OXA and NPY were colocalized in some neurons of few diencephalic areas. On the other hand, anatomical studies conducted in other fish species (Volkoff, 2016) and mammals (Sakurai, 2014) displayed that orexin and NPY neurons belong to two different sets of hypothalamic neurons, although they act synergistically (Sakurai, 2014; Volkoff & Peter, 2006). These observations shed light on possible way of interaction of the orexinergic and NPY-ergic neurons in *N. furzeri*, as components of a hypothalamic circuitry, integrating aspects of feeding behavior.

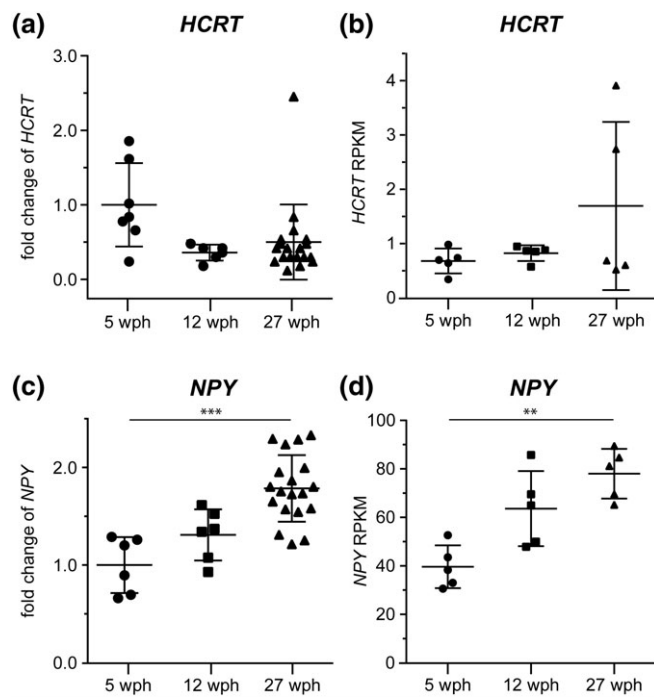## 4.2 | Age-associated regulation of HCRT and NPY in the brain of *N. furzeri*

Our data show that *HCRT* is not significantly regulated in the brain of *N. furzeri* during aging. These observations represent a great novelty in the study of vertebrates orexin system, which is characterized by an age related decline (Nixon et al., 2015), paralleled by physiological alterations in body weight regulation, sleep and locomotor activity during aging (Nixon et al., 2015). We detected slight *HCRT* decreased levels between young and adult animals, which may mirror the explosive growth of *N. furzeri* (Cellerino et al., 2016) to reach the sexual maturity (between 3 and 5 weeks). Similarly, in humans the greater loss occurs during maturation (Hunt et al., 2015).

On the other hand, *NPY* is remarkably overexpressed in the whole brain, during aging, confirming that the quantitative data matched the morphological observations. For instance, *NPY* positive neurons in the inferior lobe of hypothalamus were much more numerous in old subjects than in young. However, such enhancement of *NPY* does not fit
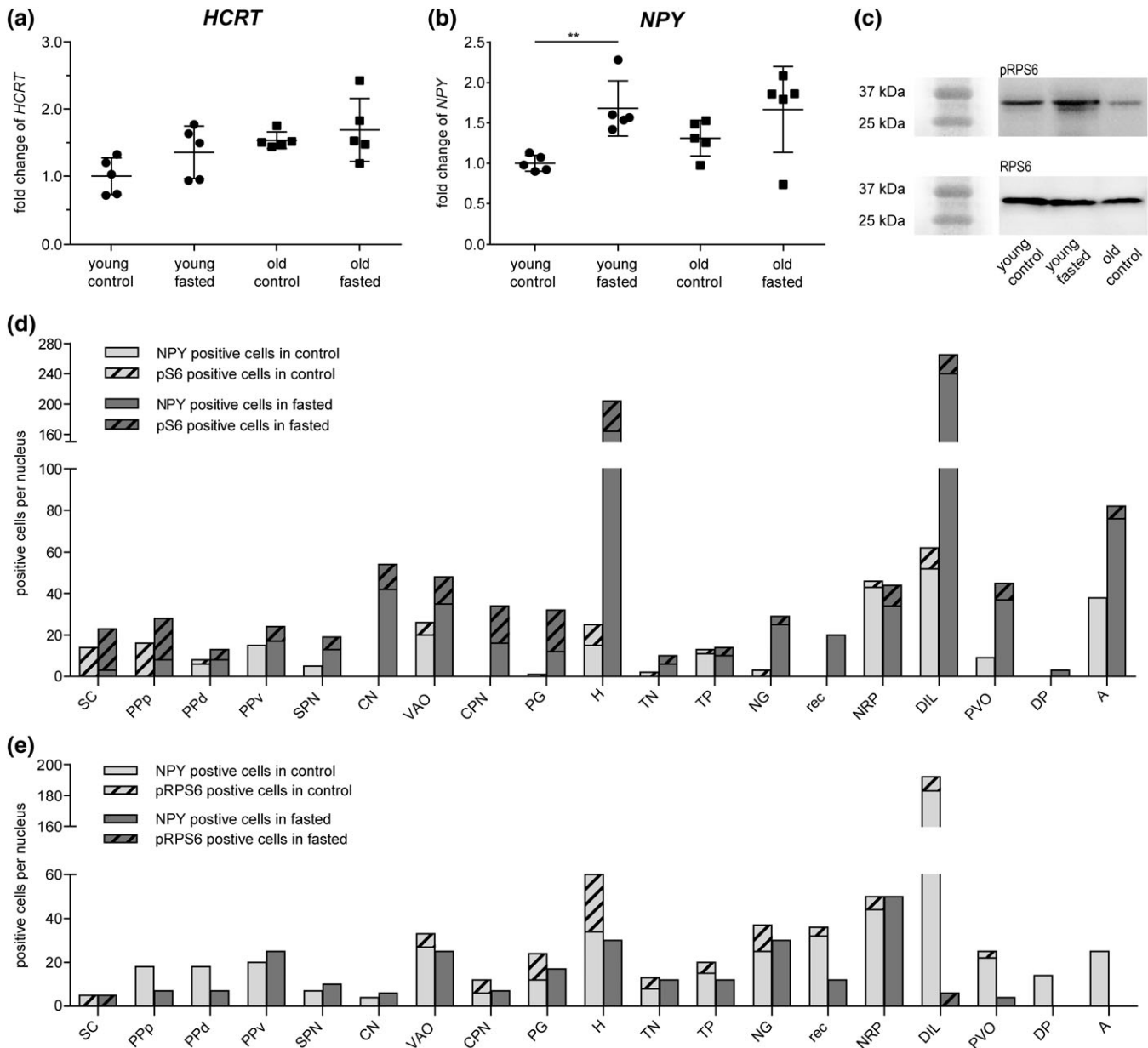
FIGURE 10 Age related regulation of *HCRT* and *NPY* by food intake in the dissected diencephalon of *N. furzeri*, in subjects at 5 wph (young, sexual maturity) and 27 wph (old). (a) Expression levels of *HCRT* in control and FA at 5 wph were not significant ($t(8) = 1.342$, $p = 1.299$, two-tailed, unpaired t test with Bonferroni's correction). (b) Expression levels of *NPY* were statistically significant in FA at 5 wph but not at 27 wph ($t(8) = 4.278$, $p = 0.0162$ two-tailed, unpaired t test with Bonferroni's correction). (c) Western blot analysis on total brain extracts of subjects at 5 wph (young, sexual maturity) and 27 wph (old), against pRPS6 and RPS6 antibodies, revealed bands of ~30 kDa. (d) Counting cells expressing *NPY* or pRPS6, the neuronal activity marker, in identified diencephalic nuclei of control and FA at 5 wph: *NPY* upregulation in 17 nuclei out of 19. pRPS6 immunoreactive cells were more numerous in FA than in controls. In SC, PPp, CPN, and PG, pRPS6 immunoreactive cells were more numerous than NPY expressing neurons. (e) Counting cells expressing *NPY* or pRPS6, in identified diencephalic nuclei of control and FA at 27 wph. *NPY* upregulation in eight nuclei of FA. pRPS6 immunoreactivity was detected only in SC and DIL of FA

with the hyperphagic phenotype (de Luca et al., 2005), because old animals tend to eat much less than adult and young. Transgenic mouse model of *NPY* overexpression and a model of conditionally overexpressed *NPY* (Thiele, Marsh, Ste Marie, Bernstein, & Palmiter, 1998) exhibited no major phenotypes related to food intake or body weight. The levels of *NPY* gene expression are generally elevated in several models of animal obesity, such as in diet-induced obesity (Guan et al., 1998), leptin-deficient ob/ob mice (Kesterson, Huszar, Lynch, Simerly, & Cone, 1997), as well as in the obese state, as shown in the Zucker rat (Dryden et al., 1995), and upon pharmacological treatments

that enhance feeding (Li and Ritter, 2004). Postmortem analysis in *N. furzeri* (Di Cicco, Tozzini, Rossi, & Cellerino, 2011) reported liver fatty degeneration up to steatosis as main degenerative lesion. Such lesions could be the consequence of the natural feeding habits (Cellerino et al., 2016), characterized by ingestion of high quantity of fatty food, as well as the spontaneous aging process. However, these lesions indicate a clear age related failure of energy homeostasis, and could contribute to the *NPY* overexpression. Interestingly, in old animals we observed a much wider pattern of *NPY* mRNA expressing neurons than in young. In the brain of old animals, we observed

positivity in nondiencephalic areas, such as optic tectum and tegmentum, and surprisingly positive NPY cells were overall numerous in all diencephalic nuclei of old control group, and very few or absent in the same nuclei of FA. This observation made us consider that NPY concurs to regulate the brain aging process of *N. furzeri*, other than the appetite control. Future experiments are mandatory to unravel the regulation of NPY in the brain of *N. furzeri* in course of aging.

4.3 | Different age related regulation of orexin and NPY by food intake

The increased number of pRPS6 positive cells confirmed that fasting activates neurons (Knight et al., 2012) in the diencephalon of *N. furzeri*, with the highest peak detected in young animals. Of the two neuropeptides, only *NPY* is significantly increased upon fasting in young animals. The increased *HCRT* levels, although not statistically significant, overlap with the pattern of *HCRT* synthesizing neurons observed in the diencephalic region. In goldfish, short-term fasting induced increased *HCRT* and *NPY* levels (Nakamachi et al., 2006), whereas in other fish species (zebrafish, winter flounder, and coho salmon) (MacDonald & Volkoff, 2010; Novak et al., 2005; Silverstein et al., 1998) long-term fasting (14 days) was associated with a significant increase in *HCRT* and *NPY*. Indeed, fish in general demonstrate a remarkable adaptation to starvation, both in controlled experiments and in their natural habitat (McCue, 2010), and we suspect an adaptive mechanism of orexin regulation in *N. furzeri*. Future experiments can help to better elucidate whether *HCRT* in *N. furzeri* is regulated by longer term fasting.

However, short-term fasting does not regulate the expression levels of the two neuropeptides in the diencephalon of old animals. Unchanged levels of *HCRT* are in good agreement with the measurements carried out either in the whole brain of old animals and in the dissected diencephalon of young animals. A key observation is represented by unregulated levels of *NPY* in the dissected diencephalon of old FA. Arguably, longer period of starvation is necessary to activate the molecular regulation of food intake in the hypothalamus of old organisms with physiological low metabolic rates.

Overall, the achieved results show that *HCRT* expression is regulated by food intake neither in young *N. furzeri* nor in aged, whereas *NPY* is regulated by food intake in young but not in old. This represents an opportunity to unravel age-related mechanisms involving NPY-ergic system, and identify potential treatment targets in the aged central nervous system of vertebrates.

CONFLICT OF INTEREST

The authors declare that they have no conflict of interest.

ORCID

Carla Lucini https://orcid.org/0000-0003-2216-6338
Livia D'Angelo https://orcid.org/0000-0001-5050-642X

REFERENCES

Alvarez, C. E., & Sutcliffe, J. G. (2002). Hypocretin is an early member of the incretin gene family. *Neuroscience Letters*, *324*(3), 169–172.

Baumgart, M., Groth, M., Priebe, S., Savino, A., Testa, G., Dix, A., ... Cellerino, A. (2014). RNA-seq of the aging brain in the short-lived fish *N. furzeri*—conserved pathways and novel genes associated with neurogenesis. *Aging Cell*, *13*(6), 965–974.

Baumgart, M., Priebe, S., Groth, M., Hartmann, N., Menzel, U., Pandolfini, L., ... Cellerino, A. (2016). Longitudinal RNA-seq analysis of vertebrate aging identifies mitochondrial complex i as a small-molecule-sensitive modifier of lifespan. *Cell Systems*, *2*(2), 122–132.

Botelho, M., & Cavadas, C. (2015). Neuropeptide Y: An anti-aging player? *Trends in Neurosciences*, *38*(11), 701–711.

Brothers, S. P., & Wahlestedt, C. (2010). Therapeutic potential of neuropeptide Y (NPY) receptor ligands. *EMBO Molecular Medicine*, *2*(11), 429–439.

Brownell, S. E., & Conti, B. (2010). Age- and gender-specific changes of hypocretin immunopositive neurons in C57Bl/6 mice. *Neuroscience Letters*, *472*(1), 29–32.

Cellerino, A., Valenzano, D. R., & Reichard, M. (2016). From the bush to the bench: The annual Nothobranchius fishes as a new model system in biology. *Biological Reviews*, *91*(2), 511–533.

Cerdá-Reverter, J. M., & Canosa, L. F. (2009). Neuroendocrine systems of the fish brain. In N. J. Bernier, G. J. Van der Kraak, A. P. Farrell, & C. J. Brauner (Eds.), *Fish neuroendocrinology* (pp. 3–74). Amsterdam, Netherlands: Elsevier.

Cerdá-Reverter, J. M., & Larhammar, D. (2000). Neuropeptide Y family of peptides: Structure, anatomical expression, function, and molecular evolution. *Biochemistry and Cell Biology—Biochimie et Biologie Cellulaire*, *78*(3), 371–392.

Cristino, L., Busetto, G., Imperatore, R., Ferrandino, I., Palomba, L., Silvestri, C., ... Di Marzo, V. (2013). Obesity-driven synaptic remodeling affects endocannabinoid control of orexinergic neurons. *Proceedings of the National Academy of Sciences of the United States of America*, *110* (24), E2229–E2238.

D'Angelo, L. (2013). Brain atlas of an emerging teleostean model: *Nothobranchius furzeri*. *Anatomical Record—Advances in Integrative Anatomy and Evolutionary Biology*, *296*(4), 681–691.

D'Angelo, L., Castaldo, L., De Girolamo, P., Lucini, C., Paolucci, M., Pelagalli, A., ... Arcamone, N. (2016a). Orexins and receptor OX2R in the gastroenteric apparatus of two teleostean species: *Dicentrarchus labrax* and *Carassius auratus*. *Anatomical Record—Advances in Integrative Anatomy and Evolutionary Biology*, *299*(8), 1121–1129.

D'Angelo, L., Lossi, L., Merighi, A., & de Girolamo, P. (2016b). Anatomical features for the adequate choice of experimental animal models in biomedicine: I. Fishes. *Annals of Anatomy—Anatomischer Anzeiger*, *205*, 75–84.

de Girolamo, P., & Lucini, C. (2011). Neuropeptide localization in nonmammalian vertebrates. *Methods in Molecular Biology*, *789*, 37–56.

de Lecea, L., & Huerta, R. (2014). Hypocretin (orexin) regulation of sleep-to-wake transitions. *Frontiers in Pharmacology*, *5*, 16.

De Lecea, L., Kilduff, T. S., Peyron, C., Gao, X. B., Foye, P. E., Danielson, P. E., ... Sutcliffe, J. G. (1998). The hypocretins: Hypothalamus-specific peptides with neuroexcitatory activity. *Proceedings of the National Academy of Sciences of the United States of America*, *95*(1), 322–327.

de Luca, C., Kowalski, T. J., Zhang, Y. Y., Elmquist, J. K., Lee, C., Kilimann, M. W., ... Chua, S. C. (2005). Complete rescue of obesity, diabetes, and infertility in db/db mice by neuron-specific LEPR-B transgenes. *Journal of Clinical Investigation*, *115*(12), 3484–3493.

Di Cicco, E., Tozzini, E. T., Rossi, G., & Cellerino, A. (2011). The short-lived annual fish *Nothobranchius furzeri* shows a typical teleost aging process reinforced by high incidence of age-dependent neoplasias. *Experimental Gerontology*, 46(4), 249–256.

Dryden, S., Pickavance, L., Frankish, H. M., & Williams, G. (1995). Increased neuropeptide Y secretion in the hypothalamic paraventricular nucleus of obese (fa/fa) Zucker rats. *Brain Research*, 690(2), 185–188.

Duarte-Neves, J., de Almeida, L. P., & Cavadas, C. (2016). Neuropeptide Y (NPY) as a therapeutic target for neurodegenerative diseases. *Neurobiology of Disease*, 95, 210–224.

Guan, X. M., Yu, H., Trumbauer, M., Frazier, E., Van der Ploeg, L. H. T., & Chen, H. (1998). Induction of neuropeptide Y expression in dorsomedial hypothalamus of diet-induced obese mice. *Neuroreport*, 9(15), 3415–3419.

Harel, I., Benayoun, B. A., Machado, B., Singh, P. P., Hu, C. K., Pech, M. F., … Brunet, A. (2015). A platform for rapid exploration of aging and diseases in a naturally short-lived vertebrate. *Cell*, 160(5), 1013–1026.

Huesa, G., van den Pol, A. N., & Finger, T. E. (2005). Differential distribution of hypocretin (orexin) and melanin-concentrating hormone in the goldfish brain. *Journal of Comparative Neurology*, 492(3), 380–381.

Hunt, N. J., Rodriguez, M. L., Waters, K. A., & Machaalani, R. (2015). Changes in orexin (hypocretin) neuronal expression with normal aging in the human hypothalamus. *Neurobiology of Aging*, 36(1), 292–300.

Inutsuka, A., & Yamanaka, A. (2013). The regulation of sleep and wakefulness by the hypothalamic neuropeptide orexin/hypocretin. *Nagoya Journal of Medical Science*, 75(1–2), 29–36.

Jennings, J. H., Rizzi, G., Stamatakis, A. M., Ung, R. L., & Stuber, G. D. (2013). The inhibitory circuit architecture of the lateral hypothalamus orchestrates feeding. *Science*, 341(6153), 1517–1521.

Kaslin, J., Nystedt, J. M., Ostergard, M., Peitsaro, N., & Panula, P. (2004). The orexin/hypocretin system in zebrafish is connected to the aminergic and cholinergic systems. *Journal of Neuroscience*, 24(11), 2678–2689.

Kessler, B. A., Stanley, E. M., Frederick-Duus, D., & Fadel, J. (2011). Age-related loss of orexin/hypocretin neurons. *Neuroscience*, 178, 82–88.

Kesterson, R. A., Huszar, D., Lynch, C. A., Simerly, R. B., & Cone, R. D. (1997). Induction of neuropeptide Y gene expression in the dorsal medial hypothalamic nucleus in two models of the Agouti obesity syndrome. *Molecular Endocrinology*, 11(5), 630–637.

Knight, Z. A., Tan, K., Birsoy, K., Schmidth, S., Garrison, J. L., Wysocki, R. W., … Friedman, J. M. (2012). Molecular profiling of activated neurons by phosphorylated ribosome capture. *Cell*, 151, 1126–1137.

Kojima, K., Kamijo, M., Kageyama, H., Uchiyama, M., Shioda, S., & Matsuda, K. (2009). Neuronal relationship between orexin-A- and neuropeptide Y-induced orexigenic actions in goldfish. *Neuropeptides*, 43(2), 63–71.

Li, A. J., & Ritter, S. (2004). Glucoprivation increases expression of neuropeptide Y mRNA in hindbrain neurons that innervate the hypothalamus. *European journal of neuroscience*. 19(8), 2147–2154.

Loh, K., Herzog, H., & Shi, Y. C. (2015). Regulation of energy homeostasis by the NPY system. *Trends in Endocrinology and Metabolism*, 26(3), 125–35.

MacDonald, E. E., & Volkoff, H. (2010). Molecular cloning and characterization of preproorexin in winter skate (*Leucoraja ocellata*). *General and Comparative Endocrinology*, 169(3), 192–196.

Matsuda, K., Azuma, M., & Kang, K. S. (2012a). Orexin system in teleost fish. *Vitamins and Hormones*, 89, 341.

Matsuda, K., Sakashita, A., Yokobori, E., & Azuma, M. (2012b). Neuroendocrine control of feeding behavior and psychomotor activity by neuropeptideY in fish. *Neuropeptides*, 46(6), 275–283.

McCue, M. D. (2010). Starvation physiology: reviewing the different strategies animals use to survive a common challenge. *Comparative Biochemistry and Physiology Part A: Molecular & Integrative Physiology*, 156(1), 1–18.

Messina, G., Dalia, C., Tafuri, D., Monda, V., Palmieri, F., Dato, A., … Monda, M. (2014). Orexin-A controls sympathetic activity and eating behavior. *Frontiers in Psychology*, 5, 997.

Meyuhas, O. (2008). Physiological roles of ribosomal protein S6: one of its kind. *International Review of Cell and Molecular Biology*, 268, 1–37.

Minor, R. K., Lopez, M., Younts, C. M., Jones, B., Pearson, K. J., Anson, R. M., … de Cabo, R. (2011). The arcuate nucleus and neuropeptide Y contribute to the antitumorigenic effect of calorie restriction. *Aging Cell*, 10(3), 483–492.

Miranda, B., Esposito, V., de Girolamo, P., Sharp, P. J., Wilson, P. W., & Dunn, I. C. (2013). Orexin in the chicken hypothalamus: Immunocytochemical localisation and comparison of mRNA concentrations during the day and night, and after chronic food restriction. *Brain Research*, 1513, 34–40.

Nakamachi, T., Matsuda, K., Maruyama, K., Miura, T., Uchiyama, M., Funaha shi, H., … Shioda, S. (2006). Regulation by orexin of feeding behaviour and locomotor activity in the goldfish. *Journal of Neuroendocrinology*, 18(4), 290–297.

Nambu, T., Sakurai, T., Mizukami, K., Hosoya, Y., Yanagisawa, M., & Goto, K. (1999). Distribution of orexin neurons in the adult rat brain. *Brain Research*, 827(1–2), 243–260.

Nixon, J. P., Mavanji, V., Butterick, T. A., Billington, C. J., Kotz, C. M., & Teske, J. A. (2015). Sleep disorders, obesity, and aging: The role of orexin. *Ageing Research Reviews*, 20, 63–73.

Nixon, J. P., & Smale, L. (2007). A comparative analysis of the distribution of immunoreactive orexin A and B in the brains of nocturnal and diurnal rodents. *Behavioral and Brain Functions*, 3, 28.

Novak, C. M., Jiang, X. L., Wang, C. F., Teske, J. A., Kotz, C. M., & Levine, J. A. (2005). Caloric restriction and physical activity in zebrafish (*Danio rerio*). *Neuroscience Letters*, 383(1–2), 99–104.

Pedrazzini, T. (2004). Importance of NPYY1 receptor-mediated pathways: Assessment using NPYY1 receptor knockouts. *Neuropeptides*, 38(4), 267–275.

Peyron, C., Tighe, D. K., van den Pol, A. N., de Lecea, L., Heller, H. C., Sutcliffe, J. G., & Kilduff, T. S. (1998). Neurons containing hypocretin (orexin) project to multiple neuronal systems. *Journal of Neuroscience*, 18(23), 9996–10015.

Rønnestad, I., Gomes, A. S., Murashita, K., Angotzi, R., Jönsson, E., & Volkoff, H. (2017). Appetite-Controlling Endocrine Systems in Teleosts. *Front Endocrinol (Lausanne)*, 8, 73.

Sakurai, T. (2014). The role of orexin in motivated behaviours. *Nature Reviews Neuroscience*, 15(11), 719–731.

Sakurai, T., Amemiya, A., Ishii, M., Matsuzaki, I., Chemelli, R. M., Tanaka, H., … Yanagisawa, M. (1998). Orexins and orexin receptors: A family of hypothalamic neuropeptides and G protein-coupled receptors that regulate feeding behavior. *Cell*, 92(4), 573–585.

Sawai, N., Ueta, Y., Nakazato, M., & Ozawa, H. (2010). Developmental and aging change of orexin-A and -B immunoreactive neurons in the male rat hypothalamus. *Neuroscience Letters*, 468(1), 51–55.

Shibahara, M., Sakurai, T., Nambu, T., Takenouchi, T., Iwaasa, H., Egashira, S. I., … Goto, K. (1999). Structure, tissue distribution, and pharmacological characterization of *Xenopus* orexins. *Peptides*, 20(10), 1169–1176.

Silverstein, J. T., Breininger, J., Baskin, D. G., & Plisetskaya, E. M. (1998). Neuropeptide Y-like gene expression in the salmon brain increases with fasting. *General and Comparative Endocrinology*, 110(2), 157–165.

Slats, D., Claassen, J. A., Verbeek, M. M., & Overeem, S. (2013). Reciprocal interactions between sleep, circadian rhythms and Alzheimer's disease: focus on the role of hypocretin and melatonin. *Ageing research reviews*, 12(1), 188–200.

Tachibana, T., & Tsutsui, K. (2016). Neuropeptide control of feeding behavior in birds and its difference with mammals. *Frontiers in Neuroscience*, 10, 485.

Terzibasi, E., Lefrancois, C., Domenici, P., Hartmann, N., Graf, M., & Cellerino, A. (2009). Effects of dietary restriction on mortality and age-related phenotypes in the short-lived fish *Nothobranchius furzeri*. *Aging Cell*, 8(2), 88–99.

Thiele, T. E., Marsh, D. J., Ste Marie, L., Bernstein, I. L., & Palmiter, R. D. (1998). Ethanol consumption and resistance are inversely related to neuropeptide Y levels. *Nature*, 396(6709), 366–369.

Tozzini, E. T., Baumgart, M., Battistoni, G., & Cellerino, A. (2012). Adult neurogenesis in the short-lived teleost *Nothobranchius furzeri*: Localization of neurogenic niches, molecular characterization and effects of aging. *Aging Cell*, 11(2), 241–251.

Tsujino, N., & Sakurai, T. (2013). Role of orexin in modulating arousal, feeding, and motivation. *Frontiers in Behavioral Neuroscience*, 7, 28.

Tsuneki, H., Sasaoka, T., & Sakurai, T. (2016). Sleep control, GPCRs, and glucose metabolism. *Trends in Endocrinology and Metabolism*, 27(9), 633–642.

Valdesalici, S., & Cellerino, A. (2003). Extremely short lifespan in the annual fish *Nothobranchius furzeri*. *Proceedings of the Royal Society B—Biological Sciences*, *270*, S189–S191.

Valenzano, D. R., Terzibasi, E., Cattaneo, A., Domenici, L., & Cellerino, A. (2006). Temperature affects longevity and age-related locomotor and cognitive decay in the short-lived fish *Nothobranchius furzeri*. *Aging Cell*, *5*(3), 275–278.

Volkoff, H. (2016). The neuroendocrine regulation of food intake in fish: A review of current knowledge. *Frontiers in Neuroscience*, *10*, 540.

Volkoff, H., & Peter, R. E. (2006). Feeding behavior of fish and its control. *Zebrafish*, *3*(2), 131–140.

Waterson, M. J., & Horvath, T. L. (2015). Neuronal regulation of energy homeostasis: Beyond the hypothalamus and feeding. *Cell Metabolism*, *22*(6), 962–970.

Wienecke, M., Werth, E., Poryazova, R., Baumann-Vogel, H., Bassetti, C. L., Weller, M., Waldvogel, D., Storch, A., & Baumann, C. R. (2012). Progressive dopamine and hypocretin deficiencies in Parkinson's disease: is there an impact on sleep and wakefulness? *Journal of Sleep Research*, *21*(6), 710–717.

Zimmerman, S. G., Peters, N. C., Altaras, A. E., & Berg, C. A. (2013). Optimized RNA ISH, RNA FISH and protein-RNA double labeling (IF/FISH) in Drosophila ovaries. *Nature Protocols*, *8*(11), 2158–2179.